Available online at www.sciencedirect.com
SCIENCE DIRECT®
International Journal of Heat and Mass Transfer 48 (2005) 1599–1607
International Journal of HEAT and MASS TRANSFER
www.elsevier.com/locate/ijhmt

Thermoacoustic streaming in a tube with isothermal outer surface

G.Q. Lu [a], P. Cheng [b,*]

[a] The Department of Mechanical and Nuclear Engineering, The Penn State University, State College, PA, 16802, USA
[b] School of Mechanical and Power Engineering, Shanghai Jiaotong University, 1954 Hua Shan Road, Shanghai, 200030, PR China

Received 5 January 2004; received in revised form 6 August 2004
Available online 1 February 2005

Abstract

Thermoacoustic oscillations at a cycle-steady state in a tube with an isothermal outer wall, and with one end closed and the other end connected to a wave generator, is analyzed based on a linearized theory. From the global mass conservation, an analytical solution has been obtained for the cross-sectional and cycle averaged axial velocity. It is shown that this averaged velocity is non-vanishing due to the mass streaming effect. By analyzing the global momentum balance, it is found that the cycle-averaged pressure depends on the momentum streaming and friction force, and a conservation relationship exists between the momentum streaming and the cycle-averaged pressure for the flow oscillating at a high frequency in a wide tube. An investigation of the global energy balance leads to an expression for thermoacoustic energy streaming. Furthermore, it is shown that the refrigeration effect is mainly caused by the non-vanishing mean velocity, and therefore the mass streaming and the energy streaming are intimately connected.

Keywords: Thermoacoustic; Streaming; Pulse tube refrigerator

1. Introduction

Pulse-tube refrigerators and thermoacoustic refrigerators are two kinds of refrigerators that share a similar refrigeration mechanism [1–3]. Based on a thermodynamic analysis, Gifford and Longsworth [4] attributed the refrigeration phenomenon to the "surface heating pumping" effect. However, in order to understand the refrigeration mechanism of a compressible oscillating flow quantatively, it is necessary to solve the governing nonlinear partial differential equations of a compressible oscillating viscous flow. To simplify the mathematical analysis, a linearized theory of thermoacoustic oscillation has been developed by Rott [5–7], Merkli and Thomann [8], Wheatley et al. [9], Swift [2,10] among others. In addition, Xiao [11], Santillan and Boullosa [12], Lu and Cheng [13], as well as Tominaga [14] have applied the linearized theory to study some aspects of thermoacoustic oscillation.

Recently, theoretical research on thermoacoustic streaming has attracted a great deal of attention since the performance of a thermoacoustic machine depends greatly on these phenomena. For example, Gopinath and Tait [15] evaluated the time-averaged temperature distribution which is the result of the energy streaming in a resonant channel. Waxler [16] and Bailliet et al.

* Corresponding author. Tel./fax: +86 21 6293 3107.
E-mail address: pingcheng@sjtu.edu.cn (P. Cheng).

0017-9310/$ - see front matter © 2004 Elsevier Ltd. All rights reserved.
doi:10.1016/j.ijheatmasstransfer.2004.08.027

[17] analyzed the mass streaming and momentum streaming by solving for the second-order physical quantities. However, discussions on the relationship between the mass streaming and the energy streaming, which is useful to understand the complex transport phenomena in thermoacoustic oscillation, have not been adequately discussed in previous work.

In this paper, we will analyze a simple case of a thermoacoustic oscillatory flow in a tube with one end closed and with outer surface at isothermal condition when the flow reaches a cycle-steady state. As in the previous work [5–10], the physical quantities are expanded in terms of a power series for small Mach numbers in the present paper. The first-order physical quantities are first solved based on the linearized equations. The cycle averaged and cross-sectional averaged axial velocity are obtained from the global mass conservation under the cycle-steady condition. Axial distribution of the cycle-averaged pressure is determined from the global momentum conservation. Local heat transfer rate along outer wall of the tube is determined analytically by analyzing the thermoacoustic energy streaming. It is shown that refrigeration effect is mainly caused by the non-vanishing mean velocity, and therefore the mass streaming and the energy streaming are connected intimately. The results given in this study are useful to understand the refrigeration mechanism in a thermoacoustic refrigerator and a basic pulse-tube refrigerator.

2. Assumptions and simplified governing equations

Consider thermoacoustic oscillation in a tube with length L, outer radius R_o and inner radius R_i as shown in Fig. 1. One end ($X = 0$) of this tube is driven by a pressure generator (such as a piston) while the other end ($X = L$) is closed. The outer surface of this tube is isothermal. The piston is oscillating with an amplitude of the axial velocity u_d and a frequency ω.

We assume that the thermoacoustic oscillation in this tube has reached a cycle-steady state where the oscillation is stable. In particular, we assume that the local heat transfer between the outer isothermal wall of the tube and its surrounding environment matches with the local heat transfer rate of the fluid at the inner wall so that the oscillation is maintained at a cycle-steady state. The value of this local heat transfer rate between the outer wall and its surroundings is determined analytically in this paper, which can be used to explain the refrigeration mechanism occurring in a thermoacoustic machines.

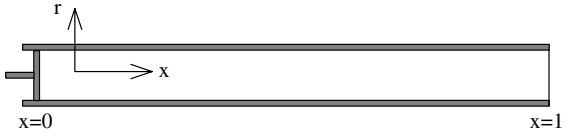

Fig. 1. Schematic diagram of a tube.

Furthermore, we assume that (1) the oscillation occurs in a sufficiently long tube, (2) the driven oscillating frequency is high (i.e., near a resonant condition, but avoiding a shock wave occurring), and (3) the oscillatory amplitude of the velocity is small at the driven end, i.e.

$$\frac{R_i}{L} \ll 1, \quad \frac{\omega L}{a} \propto 1, \quad M = \frac{u_d}{a} \ll 1 \tag{1a–c}$$

where M is Mach number, and $a = \sqrt{\gamma R T_0}$ is sound speed with R being the gas constant and γ the ratio of specific heats. T_0 and p_0 are reference temperature and pressure, which are defined as the volume-averaged and cycle-averaged temperature and pressure in the system at a cycle-steady state, respectively, and therefore are independent of spatial and temporal coordinates.

The governing equations for the oscillating flow in an axisymmetric cylindrical coordinate can be normalized by scaling temperature by T_0, pressure by p_0, density by $\rho_0 = p_0/(RT_0)$, axial velocity by sound speed a, radial velocity by aR_i/L, axial coordinate by L, radial coordinate by R_i and time coordinate by $1/\omega$. The normalized governing equations for a compressible flow in an axisymmetric coordinate are:

$$\frac{\partial \rho}{\partial t} + \frac{a}{\omega L}\left[\frac{1}{r}\frac{\partial}{\partial r}(\rho v r) + \frac{\partial}{\partial x}(\rho u)\right] = 0 \tag{2}$$

$$\begin{aligned}\rho\left[\frac{\partial u}{\partial t} + \frac{a}{\omega L}\left(u\frac{\partial u}{\partial x} + v\frac{\partial u}{\partial r}\right)\right] &= -\frac{a}{\gamma \omega L}\frac{\partial p}{\partial x} + \frac{\upsilon}{\omega R_i^2}\frac{1}{r}\frac{\partial}{\partial r}\left(r\frac{\partial u}{\partial r}\right) \\ &\quad + \frac{R_i^2}{L^2}\left\{\frac{4}{3}\frac{\upsilon}{\omega R_i^2}\frac{\partial^2 u}{\partial x^2} + \frac{1}{3}\frac{\upsilon}{\omega R_i^2}\frac{\partial}{\partial x}\left[\frac{1}{r}\frac{\partial}{\partial r}(rv)\right]\right\}\end{aligned} \tag{3}$$

$$\frac{\partial p}{\partial r} = \mathrm{O}\left(\frac{R_i^2}{L^2}\right) \quad \text{or} \quad p = p(x,t) \tag{4a, b}$$

$$\begin{aligned}\rho\left[\frac{\partial T}{\partial t} + \frac{a}{\omega L}\left(u\frac{\partial T}{\partial x} + v\frac{\partial T}{\partial r}\right)\right] &= \frac{\gamma - 1}{\gamma}\left[\frac{\partial p}{\partial t} + \frac{a}{\omega L}\left(u\frac{\partial p}{\partial x} + v\frac{\partial p}{\partial r}\right)\right] \\ &\quad + \frac{1}{\omega C_p \rho_0 R_i^2}\frac{1}{r}\frac{\partial}{\partial r}\left(kr\frac{\partial T}{\partial r}\right) \\ &\quad + \frac{R_i^2}{L^2}\left[\frac{1}{\omega C_p \rho_0 R_i^2}\frac{\partial}{\partial x}\left(k\frac{\partial T}{\partial x}\right)\right] + \mathrm{O}\left(\frac{R_i^2}{L^2}\right)\end{aligned} \tag{5}$$

$$\begin{aligned}\frac{\partial T_s}{\partial t} &= \frac{1}{\omega \rho_s C_{p,s} R_i^2}\frac{1}{r}\frac{\partial}{\partial r}\left(k_s r\frac{\partial T_s}{\partial r}\right) \\ &\quad + \frac{R_i^2}{L^2}\left[\frac{1}{\omega \rho_s C_{p,s} R_i^2}\frac{\partial}{\partial x}\left(k_s\frac{\partial T_s}{\partial x}\right)\right]\end{aligned} \tag{6}$$

$$p = \rho T \tag{7}$$

Eqs. (2)–(7) are the continuity equation, Navier-Stokes equations, energy equations for the fluid and the solid phase (i.e., the wall) as well as the state equation, respectively. In these equations, the coefficients μ, C_p and k denote the viscosity, specific heat and thermal conductivity, respectively. The subscript "s" denotes the quantity associated with solid phase (or the wall). According to the long tube assumption given in Eq. (1a), viscous effect due to the axial gradient indicated by the last braces term in the in Eq. (3) can be neglected. Similarly, heat conduction due to the axial temperature gradients in Eqs. (5) and (6) and the dissipation terms in Eq. (5) can also be neglected. Furthermore, radial momentum equation can be neglected, thus pressure is independent of radial coordinate as shown in Eq. (4).

In the present problem, thermoacoustic oscillation is introduced by a pressure generator, which has a small oscillatory amplitude and its Mach number is much smaller than unity as indicated in Eq. (1c). We now expand the transient physical quantities into a perturbation series in terms of the small parameter M, the Mach number. For example, the normalized axial velocity, normalized pressure and normalized temperature can be expressed as:

$$u(x,r,t) = \left\{\frac{1}{2}\left[u_1(x,r)e^{it} + u_1^*(x,r)e^{-it}\right]\right\}M + \left\{u_{20}(x,r) + \frac{1}{2}\left[u_2(x,r)e^{2it} + u_2^*(x,r)e^{-2it}\right]\right\}M^2 + \cdots \tag{8a}$$

$$p(x,t) = 1 + \left\{\frac{1}{2}\left[p_1(x)e^{it} + p_1^*(x)e^{-it}\right]\right\}M + \left\{p_{20}(x) + \frac{1}{2}\left[p_2(x)e^{2it} + p_2^*(x)e^{-2it}\right]\right\}M^2 + \cdots \tag{8b}$$

$$T(x,r,t) = 1 + \left\{\frac{1}{2}\left[T_1(x,r)e^{it} + T_1^*(x,r)e^{-it}\right]\right\}M + \left\{\frac{1}{2}\left[T_2(x,r)e^{2it} + T_2^*(x,r)e^{-2it}\right]\right\}M^2 + \cdots \tag{8c}$$

where i is a unit complex quantity. The superscript "*" indicates complex conjugate and the subscripts "1" and "2" stand for the first-order term and second-order term, respectively. In Eq. (8), conjugate terms e^{-it} and e^{-2it} are included so that both sides of the equations are real numbers. The Fourier expansion series in the form of Eq. (8) can always be carried out if the quantities are cycle-repeatable and mathematically continuous functions with respect to time. In Eq. (8a), u_{20} is cycle-averaged normalized axial velocity. Eq. (8b) is independent of r because of the long tube assumption given by Eq. (4b). In addition, p_{20} in Eq. (8b) is the percentage deviation of cycle-averaged local pressure with respect to p_0. u_{20} and p_{20} are of second-order in amplitude because they are caused by the fluctuations of the first-order quantities. Note that $T_{20} = 0$ in Eq. (8c) because we have assumed that the thermoacoustic oscillation occurs in a tube whose outer surface is isothermal due to efficient heat exchange with surroundings. Thus, the present problem is different from that of thermoacoustic oscillation in an adiabatic tube where the oscillation will eventually build up a cycle-steady state temperature gradient [15–17].

We now substitute Eq. (8) into the governing equations given by Eq. (2)–(7), and collect first-order terms. Note that we can collect separately the coefficients of e^{it} and e^{-it} because these quantities vary with respect to time independently. It is noted that the coefficient equations of e^{it} and e^{-it} are complex conjugate of each other. For this reason, we need only to work with one set of equations. The resultant normalized first-order governing equations for thermoacoustic oscillation in an axisymmetric tube are given below:

$$i\rho_1 + \frac{a}{\omega L}\left[\frac{1}{r}\frac{\partial}{\partial r}(v_1 r) + \frac{\partial u_1}{\partial x}\right] = 0 \tag{9}$$

$$iu_1 = -\frac{a}{\gamma\omega L}\frac{\partial p_1}{\partial x} + \frac{\delta_v^2}{2R_i^2}\frac{1}{r}\frac{\partial}{\partial r}\left(r\frac{\partial u_1}{\partial r}\right) \tag{10}$$

$$iT_1 = \frac{\gamma - 1}{\gamma} ip_1 + \frac{\delta_t^2}{2R_i^2}\frac{1}{r}\frac{\partial}{\partial r}\left(r\frac{\partial T_1}{\partial r}\right) \tag{11}$$

$$iT_{s,1} = \frac{\delta_s^2}{2R_i^2}\frac{1}{r}\frac{\partial}{\partial r}\left(r\frac{\partial T_{s,1}}{\partial r}\right) \tag{12}$$

$$p_1 = T_1 + \rho_1 \tag{13}$$

with radial boundary conditions given by:

$$r = 0: \quad \frac{\partial u_1}{\partial r} = 0, \ \frac{\partial v_1}{\partial r} = 0, \ \frac{\partial T_1}{\partial r} = 0 \tag{14a–c}$$

$$r = 1: \quad u_1 = 0, \ v_1 = 0, \ T_1 = T_{s,1}, \ k_0\frac{\partial T_1}{\partial r} = k_{s,0}\frac{\partial T_{s,1}}{\partial r} \tag{15a–d}$$

$$r = 1 + \Delta: \quad T_{s,1} = 0 \tag{16}$$

The characteristic dimensionless quantities in Eqs. (9)–(13) are defined as: $\delta_v = (2\mu_0/\omega\rho_0)^{1/2}$ is the fluid's viscous penetration depth; $\delta_t = (2k_0/\omega\rho_0 C_{p,0})^{1/2}$ is the fluid's thermal penetration depth; $\delta_s = (2k_{s,0}/\omega\rho_{s,0}C_{p,s,0})^{1/2}$ is the solid's thermal penetration depth; and $\Delta = R_o/R_i$ is a geometrical parameter of the tube. Boundary conditions given by Eq. (15c) and (15d) are the matching conditions at the fluid-solid interface while Eq. (16) is for an isothermal outer wall.

3. Radial distributions of the first-order quantities

Radial distribution of the normalized first-order physical quantities governing by Eqs. (9)–(16) can be determined analytically. The radial solutions for these normalized first-order quantities are:

$$u_1 = -\frac{a}{\mathrm{i}\gamma\omega L}\frac{\mathrm{d}p_1}{\mathrm{d}x}\left[1-\frac{J_0(\eta)}{J_0(\eta_0)}\right] \tag{17}$$

$$T_1 = \frac{\gamma-1}{\gamma}\left[1-\frac{1}{1-b_3}\frac{J_0(\sigma\eta)}{J_0(\sigma\eta_0)}\right]p_1 \tag{18}$$

$$\rho_1 = \frac{\gamma-1}{\gamma}\left[\frac{1}{\gamma-1}+\frac{1}{1-b_3}\frac{J_0(\sigma\eta)}{J_0(\sigma\eta_0)}\right]p_1 \tag{19}$$

where the coefficient b_3 is given by

$$b_3 = \frac{1}{\varepsilon}\frac{\dfrac{J_1(\sigma\eta_0)}{J_0(\sigma\eta_0)}\left[\dfrac{Y_0(\sigma_s\Delta\eta_0)}{J_0(\sigma_s\Delta\eta_0)}-\dfrac{Y_0(\sigma_s\eta_0)}{J_0(\sigma_s\eta_0)}\right]}{\dfrac{J_1(\sigma_s\eta_0)}{J_0(\sigma_s\eta_0)}\left[\dfrac{Y_0(\sigma_s\Delta\eta_0)}{J_0(\sigma_s\Delta\eta_0)}-\dfrac{Y_1(\sigma_s\eta_0)}{J_1(\sigma_s\eta_0)}\right]} \tag{20}$$

In the above equations, the variable $\eta = \eta_0 r$ with $\eta_0 = (\mathrm{i}-1)R_\mathrm{i}/\delta_\mathrm{v}$ being the dimensionless radial coordinate. $J_j(\eta)$ is the Bessel function of the first kind of order j and $Y_j(\eta)$ is the Bessel function of the second kind of order j. $\sigma = Pr^{1/2} = (\mu_0 C_{\mathrm{p},0}/k_0)^{1/2} = \delta_\mathrm{v}/\delta_\mathrm{t}$ is the square root of Prandtl number, which is the ratio of the fluid's viscous penetration depth to thermal penetration depth; $\sigma_\mathrm{s} = \delta_\mathrm{v}/\delta_\mathrm{s}$ is the ratio of the fluid's viscous penetration depth to the solid's thermal penetration depth; $\varepsilon = \frac{k_{\mathrm{s},0}\delta_\mathrm{t}}{k_0\delta_\mathrm{s}} = \frac{\dot{q}\delta_\mathrm{t}/k_0}{\dot{q}\delta_\mathrm{s}/k_{\mathrm{s},0}} \equiv \frac{\Theta_\mathrm{f}}{\Theta_\mathrm{s}}$ is a parameter denoting the ratio of temperature difference across the fluid's penetration depth to that of the solid's penetration depth. One should note that the solution of temperature given in Eq. (18) is somewhat different from that of Rott's [7] or Merkli and Thomann's [8] because different thermal boundary conditions were used. Consequently, axial distributions of the first-order quantities, which will be given in the following section, are also different from that given by Merkli and Thomann's [8]. Eqs. (17)–(19) with different scaling parameters were also derived independently by Swift [18].

4. Axial distributions of the cross-sectional averaged first-order quantities

We now define the cross-section area average quantities as $\overline{\Omega} = \frac{1}{A_0}\int_{A_0}\Omega\,\mathrm{d}A$ with A_0 being the cross-section area. Substituting the first-order velocity given by Eq. (17) into the above expression, we obtain the following first-order cross-sectional averaged velocity:

$$\bar{u}_1 = -\frac{a}{\mathrm{i}\gamma\omega L}\frac{\mathrm{d}p_1}{\mathrm{d}x}\left[1-\frac{2}{\eta_0}\frac{J_1(\eta_0)}{J_0(\eta_0)}\right] \tag{21}$$

In addition, we can integrate the continuity equation given by Eq. (9) over the cross-sectional area and take note of the radial boundary conditions to give

$$\mathrm{i}\bar{\rho}_1 + \frac{a}{\omega L}\frac{\partial\bar{u}_1}{\partial x} = 0 \tag{22}$$

Integrating the first-order density given by Eq. (19) and substituting the resultant equation in Eq. (22) to give

$$\left[\frac{1}{\gamma}+\frac{\gamma-1}{\gamma}\frac{1}{1-b_3}\frac{2}{\sigma\eta_0}\frac{J_1(\sigma\eta_0)}{J_0(\sigma\eta_0)}\right]p_1 + \frac{a}{\mathrm{i}\omega L}\frac{\partial\bar{u}_1}{\partial x} = 0 \tag{23}$$

Differentiating Eq. (23) with respect to x and substituting the cross-sectional averaged velocity given by Eq. (21) in the resulting equation to eliminate the p_1 term, we can obtain an axial governing equation for $\bar{u}_1$:

$$\frac{\partial^2\bar{u}_1}{\partial x^2} - c^2\bar{u}_1 = 0 \tag{24}$$

where the coefficient c is given by

$$c^2 = -\frac{1+\dfrac{\gamma-1}{1-b_3}\dfrac{2}{\sigma\eta_0}\dfrac{J_1(\sigma\eta_0)}{J_0(\sigma\eta_0)}}{1-\dfrac{2}{\eta_0}\dfrac{J_1(\eta_0)}{J_0(\eta_0)}}\left(\frac{\omega L}{a}\right)^2 \tag{25}$$

Since one end of the tube is closed while the other end is connected to a driving pressure wave generator, as shown in Fig. 1, axial boundary conditions for Eq. (24) are given by:

$$x = 0: \ \bar{u}_1(x) = 1 \quad \text{and} \quad x = 1: \ \bar{u}_1(x) = 0 \tag{26a, b}$$

where we have chosen original point of time coordinate so that the phase angle of the oscillation of the velocity is zero at the driven end ($x = 0$). Consequently:

$$\bar{u}_1(x) = \frac{\mathrm{e}^{cx} - \mathrm{e}^{2c-cx}}{1-\mathrm{e}^{2c}} \tag{27}$$

Eq. (27) gives a complex number where its modulus gives the fluctuation amplitude and its phase angle indicating the phase shift of the fluctuation with respect to a reference wave (which is defined as the velocity wave at the driven end). In addition, the normalized first-order pressure can be obtained as:

$$p_1(x) = \frac{\mathrm{i}c}{\dfrac{1}{\gamma}+\dfrac{\gamma-1}{\gamma}\dfrac{1}{1-b_3}\dfrac{2}{\sigma\eta_0}\dfrac{J_1(\sigma\eta_0)}{J_0(\sigma\eta_0)}}\frac{\mathrm{e}^{cx}+\mathrm{e}^{2c-cx}}{1-\mathrm{e}^{2c}}\left(\frac{a}{\omega L}\right) \tag{28}$$

It should be noted that mathematical singular points appear in both Eqs. (27) and (28) when the coefficient c approaches the limit of $\mathrm{i}n\pi$ with n being a positive integer. In such a case, the denominators in Eqs. (27) and (28) approach to zero values. Consequently, velocity and pressure approach to infinite values. Physically, resonant oscillation will occur when this singular point is approached by increasing the oscillatory frequency, and a shock wave may arise as a result. Consider the

limiting case of $R_i/\delta_v \to \infty$ (i.e., a tube with a large radius in comparison with the viscous penetration depth) hence $\eta_0 = (i-1)R_i/\delta_v \to \infty$. From Eq. (25), we can obtain $c = \pm\omega Li/a$ for such a tube. Abandoning the negative value of c as being physically unrealistic, we have the expression for this singular point in Eq. (27) or Eq. (28) as $\omega L/a = n\pi$. It follows that $\omega = \pi a/L$ is the intrinsic resonant angular frequency in a large diameter tube with a length of L.

Numerical calculations for Eqs. (27) and (28) were carried out for the nearly resonant condition of $\omega L/a = 0.95\pi$ under the following conditions: the solid phase is stainless steel, $\Delta = 1.05$, $R_i/\delta_v = 50$, $T_0 = 300$ K, $p_0 = 1$ MPa. The working fluid may either be the helium gas (with $Pr = 0.667$, $\gamma = 1.667$, $\varepsilon = 206.570$, $\sigma_s = 1.724$) or the nitrogen gas (with $Pr = 0.714$, $\gamma = 1.4$, $\varepsilon = 425.850$, $\sigma_s = 0.618$). The results of the computations are presented in Figs. 2–5.

Fig. 2 gives the axial distribution of fluctuation amplitude of first-order pressure along the tube where it is shown that the minimum value of p_1 occurs near the center of the tube when oscillation frequency is at nearly resonant condition. Fig. 3 gives the phase angles of first-order pressure along the axial position which has a sudden drop near the center of the tube. Figs. 4 and 5 give the axial distribution of fluctuation amplitude of first-order velocity and its phase angle along the axial location. Fig. 4 shows that the fluctuation amplitude of the first-order velocity reaches a maximum value near the axial center of the tube when oscillation frequency is at a nearly resonant condition. Fig. 5 shows the phase angle of velocity at any axial location lagging behind the induced velocity at the driven end of the tube. Comparing with the phase angles of the pressure and of the velocity shown in Figs. 3 and 5, one can conclude that oscillations of both helium gas and nitrogen gas are slightly different from the standing wave pattern since the phase shift between the velocity and the pressure are not equal to 90° exactly. For the same reduced frequency $\omega L/a$ and reduced geometrical size R_i/δ_v, it is shown in Figs. 2 and 4 that the helium gas has larger fluctuation amplitudes of the pressure and the velocity compared with those of the nitrogen gas. This is because the helium gas has a smaller Prandtl number [8].

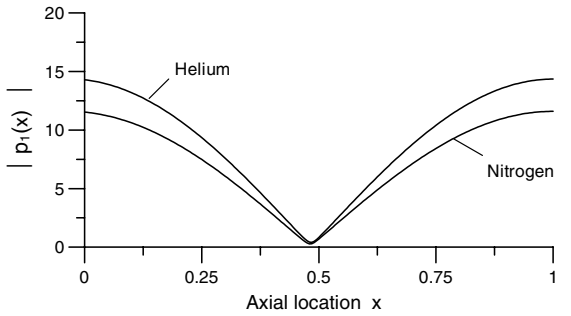

Fig. 2. Axial distribution of fluctuation amplitude of the first-order pressure.

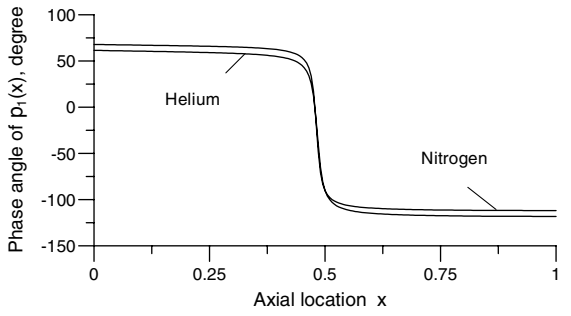

Fig. 3. Axial distribution of the phase angle of first-order pressure.

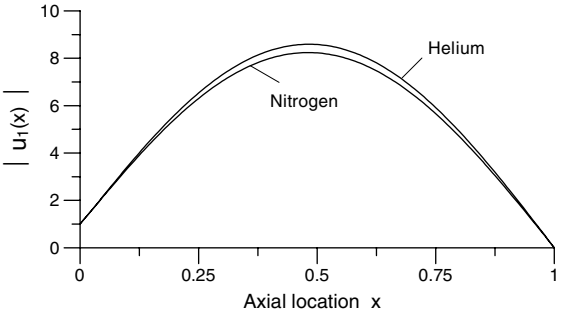

Fig. 4. Axial distribution of the fluctuation amplitude of first-order velocity.

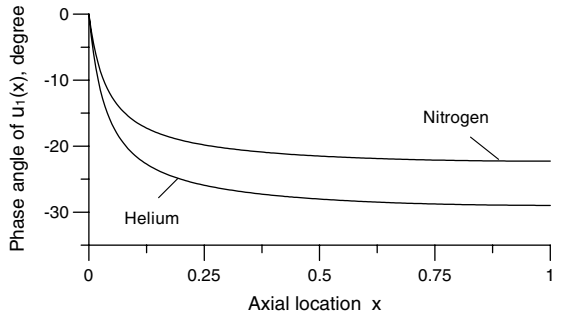

Fig. 5. Axial distribution of the phase angle of first-order velocity.

5. Thermoacoustic mass streaming and axial velocity $\bar{u}_{20}$

Integrating Eq. (2) over a cycle, the first term of Eq. (2) will vanish since cycle-averaged density should be a constant and fluctuation of the density will be cycle-repeatable at a cycle-steady state. Further cross-sectional averaging of Eq. (2), with the radial velocity being zero at the wall taken into consideration, gives

$$\frac{\partial}{\partial x}\overline{\langle \rho u\rangle} = 0 \quad \text{or} \quad \overline{\langle \rho u\rangle} = 0 \tag{29a, b}$$

where braces denote cycle average and the overbar indicates cross-sectional average. Eq. (29b) is obtained from Eq. (29a) by imposing the mass flow rate is zero at the closed end of the tube. In fact, Eq. (29b) shows that the net mass flux is zero everywhere in the tube.

Substituting the perturbation series of the density and axial velocity in Eq. (29b) and collecting the second-order terms while neglecting higher-order terms give

$$\bar{u}_{20}M^2 + \frac{1}{4}\left[\overline{\rho_1 u_1^*} + \overline{\rho_1^* u_1}\right]M^2 = 0$$

or

$$\bar{u}_{20} = -\frac{1}{2}\Re\left[\overline{\rho_1 u_1^*}\right] \tag{29c,d}$$

where $\Re$ signifies the real part of a complex number. The last term in Eq. (29d) is due to the fluctuations of the density and velocity, which is called the thermoacoustic mass streaming. Eq. (29d) indicates that there is a non-vanishing cycle-averaged and cross-sectional averaged axial velocity $\bar{u}_{20}$ which is caused by the thermoacoustic mass streaming. From Eq. (29d), we also can conclude that $\bar{u}_{20} = 0$ for an incompressible oscillating flow where the fluctuation of the density $\rho_1 = 0$.

Substituting Eqs. (17) and (19) in Eq. (29d) gives:

$$\bar{u}_{20} = \frac{\gamma - 1}{2\gamma^2}\frac{a}{\omega L}\Re\left[\bar{f}_1 p_1 \frac{\mathrm{d}p_1^*}{\mathrm{d}x}\right] \tag{30}$$

with the coefficient f_1 given by:

$$f_1 = \mathrm{i}\left[1 - \frac{J_0(\eta^*)}{J_0(\eta_0^*)}\right]\left[\frac{1}{\gamma - 1} + \frac{1}{1 - b_3}\frac{J_0(\sigma\eta)}{J_0(\sigma\eta_0)}\right] \tag{31}$$

The normalized $\bar{u}_{20}$ given by Eq. (30) was computed for the helium gas and the results are presented in Fig. 6. It is shown that the value of $\bar{u}_{20}$ is zero at the closed end (at $x = 1$) and has a negative value elsewhere. It is worthy of noting that $\bar{u}_{20}$ is the cycle averaged and cross-sectional averaged axial velocity at the cycle-steady state, which is different from the concept of secondary flow and the DC flow.

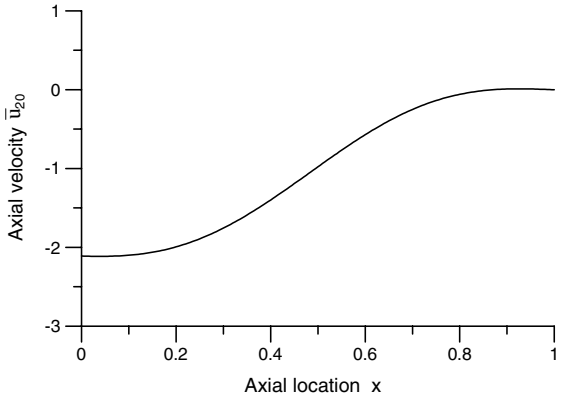

Fig. 6. Cross-sectional and cycle averaged axial velocity.

6. Thermoacoustic momentum streaming and cycle-averaged pressure

Rewriting the axial momentum equation of Eq. (3) in a conservation form, we have:

$$\frac{\partial(\rho u)}{\partial t} + \frac{a}{\omega L}\left[\frac{\partial(\rho u^2)}{\partial x} + \frac{1}{r}\frac{\partial}{\partial r}(r\rho uv)\right] = -\frac{a}{\gamma\omega L}\frac{\partial p}{\partial x} + \frac{\delta_v^2}{2R_i^2}\frac{1}{r}\frac{\partial}{\partial r}\left(r\frac{\partial u}{\partial r}\right) \tag{32}$$

If we perform a cycle average and cross-sectional average of the above equation, taking into consideration of the boundary condition that velocity being zero at the wall, we obtain:

$$\frac{a}{\omega L}\frac{\partial\overline{\langle \rho u^2\rangle}}{\partial x} = -\frac{1}{\gamma}\frac{a}{\omega L}\frac{\partial\langle p\rangle}{\partial x} + \frac{\delta_v^2}{R_i^2}\left\langle\left(\frac{\partial u}{\partial r}\right)_{r=1}\right\rangle \tag{33}$$

Eq. (33) gives a constraining condition for the cycle balance of the momentum transfer at a cycle-steady state, where $\overline{\langle \rho u^2\rangle}$ is the thermoacoustic momentum streaming which is due to the fluctuation of the momentum and has a non-vanishing cycle effect. Note that the second term of Eq. (33) denotes the cycle-averaged pressure gradient and the last term signifies the friction force due to the viscous effect.

The friction force is confined within the viscous penetration depth. If the radius of tube is much larger than the viscous penetration depth, this viscous term in Eq. (33) can be neglected. Consequently, the local cycle-averaged pressure and local thermoacoustic momentum streaming have a conservation relationship $\frac{1}{\gamma}\langle p\rangle + \overline{\langle \rho u^2\rangle} = \text{constant}$. This conservation relation has a form similar to the Bernoulli equation for a steady inviscous flow. Substituting the perturbation series of physical quantities in this conservation relation, after some mathematically manipulations, we have:

$$p_{20}(x) = \int_0^1 \left[\frac{1}{2\gamma}\left(\frac{a}{\omega L}\right)^2\left|\frac{\mathrm{d}p_1}{\mathrm{d}x}\right|^2 f_2\right]\mathrm{d}x - \frac{1}{2\gamma}\left(\frac{a}{\omega L}\right)^2\left|\frac{\mathrm{d}p_1}{\mathrm{d}x}\right|^2 f_2 \tag{34}$$

where

$$f_2 = \overline{\left|1 - \frac{J_0(\eta)}{J_0(\eta_0)}\right|^2} \tag{35}$$

where the operator $|\cdot|$ stands for the modulus of a complex number which indicates the fluctuation amplitude

of a physical quantity. The non-vanishing cycle-averaged and cross-sectional averaged pressure gradient in a pulse tube refrigerator has been verified by experimental and numerical results [19,20].

7. Thermoacoustic energy streaming and local heat transfer rate

Writing the energy equation (5) in a conservation form and neglecting the thermal dissipation terms due to the viscous work, we have:

$$\frac{\partial(\rho T)}{\partial t}+\frac{a}{\omega L}\left[\frac{\partial(\rho u T)}{\partial x}+\frac{1}{r}\frac{\partial(r\rho v T)}{\partial r}\right] = \frac{\gamma-1}{\gamma}\left(\frac{\partial p}{\partial t}+\frac{a}{\omega L}u\frac{\partial p}{\partial x}\right)+\frac{1}{\omega C_p\rho_0 R_i^2}\frac{1}{r}\frac{\partial}{\partial r}\left(kr\frac{\partial T}{\partial r}\right) + \frac{R_i^2}{L^2}\left[\frac{1}{\omega C_p\rho_0 R_i^2}\frac{\partial}{\partial x}\left(k\frac{\partial T}{\partial x}\right)\right] \tag{36}$$

Next we perform a cycle-averaging and cross-sectional averaging of energy equations for the fluid given by Eq. (36) and for the wall given by Eq. (6). Adding the two resultant equations together leads to the following cycle balanced energy equation:

$$\frac{a}{\omega L}\frac{\partial\overline{\langle\rho u T\rangle}}{\partial x}=\frac{\gamma-1}{\gamma}\frac{a}{\omega L}\left\langle\bar{u}\frac{\partial p}{\partial x}\right\rangle + \frac{2\Delta}{\omega C_p\rho_0 R_i^2}\left\langle k_s\left(\frac{\partial T_s}{\partial r}\right)_{r=\Delta}\right\rangle \tag{37}$$

The first term at the right-hand side of Eq. (37) stands for the variation of the kinetic energy during a cycle, which was neglected in the classical thermoacoustic theory.

The last term in Eq. (37) signifies the heat transfer between the outer wall of the tube and its surrounding environment. The local dimensionless heat transfer rate at the outer wall is given by:

$$q\equiv-\frac{L}{a}\frac{\gamma}{\gamma-1}\frac{2\Delta}{C_p\rho_0 R_i^2}\left\langle k_s\left(\frac{\partial T_s}{\partial r}\right)_{r=\Delta}\right\rangle = -\frac{\gamma}{\gamma-1}\frac{\partial\overline{\langle\rho u T\rangle}}{\partial x}+\left\langle\bar{u}\frac{\partial p}{\partial x}\right\rangle \tag{38}$$

where heat is transferred from the fluid if q is positive, and is absorbed by the fluid if q is negative. The expression of the energy streaming $\overline{\langle\rho u T\rangle}$ in Eq. (38) has been given by Merkli and Thomann [8] as well as by Rott [6]. A simpler expression for $\overline{\langle\rho u T\rangle}$ can be deduced as follows. By substituting the normalized state equation for an ideal gas $p=\rho T$, we have $\overline{\langle\rho u T\rangle}=\langle p\bar{u}\rangle$, where p is independent of radial location due to long tube assumption. This expression of the energy streaming can be applied to any oscillation flow as long as the working fluid is an ideal gas.

Substituting the perturbation series of the pressure and velocity in Eq. (38) and collecting the second-order terms while neglecting higher-order terms lead to:

$$Q\equiv\frac{q}{M^2}=Q_a+Q_b+Q_c \tag{39}$$

where

$$Q_a=-\frac{\gamma}{\gamma-1}\frac{\partial\bar{u}_{20}}{\partial x}$$

$$Q_b=-\frac{\gamma}{2(\gamma-1)}\frac{\partial}{\partial x}\left[\Re\overline{\langle p_1 u_1^*\rangle}\right] =-\frac{1}{2(\gamma-1)}\frac{a}{\omega L}\Re\left[f_3 p_1^*\frac{d^2p_1}{dx^2}+f_3\left|\frac{dp_1}{dx}\right|^2\right] \tag{40a–c}$$

$$Q_c=\frac{1}{2}\Re\left[\left\langle\bar{u}_1\frac{dp_1^*}{dx}\right\rangle\right]=\frac{1}{2\gamma}\frac{a}{\omega L}\left|\frac{dp_1}{dx}\right|^2\Re[f_3]$$

with the coefficient f_3 given by:

$$f_3=i-\frac{2i}{\eta_0}\frac{J_1(\eta_0)}{J_0(\eta_0)} \tag{41}$$

Eq. (39) indicates that the normalized local heat transfer rate q consists of three terms: Q_a is the local heat flux caused by non-vanishing cycle-averaged axial velocity; Q_b is the local acoustic work due to the oscillation of the first-order pressure and axial velocity; and Q_c is the local work due to the pressure gradient which signifies the variation of the kinetic energy during an oscillatory cycle. Note that the sum of Q_a and Q_b is caused by the axial gradient of the thermoacoustic energy streaming, and we may refer the sum of these two terms as the local energy streaming. Note also that $Q_a=0$ for an incompressible flow for which $\bar{u}_{20}=0$.

Fig. 7 gives the axial distributions of Q, Q_a, Q_b and Q_c for a helium gas. It is shown that Q_a has a negative value at most of axial locations. As discussed in the foregoing paragraphs, there is a non-vanishing $\bar{u}_{20}$ caused by the mass streaming. Physically, the term Q_a stands for the energy needed to drive the axial gradient of this non-vanishing velocity. The distribution of the local acoustic work Q_b is also given in Fig. 7. It is easy to understand that this local acoustic work is positive since the input of mechanical work is needed in order to maintain the thermoacoustic oscillation. This local acoustic work will dissipate into heat during the oscillation cycle. In addition, the local work due to the variation of the kinetic energy Q_c is also presented in Fig. 7. Note that $Q_c<0$ along the axial direction, which signifies the loss of the kinetic energy during a cycle due to the friction effect. This local kinetic energy loss Q_c has to be compensated by the input of acoustic work or heat. The total local heat transfer rate Q, consisting of local heat flux Q_a, thermal energy dissipated by local inputted acoustic work Q_b, and local kinetic energy loss Q_c, is also presented in Fig. 7.

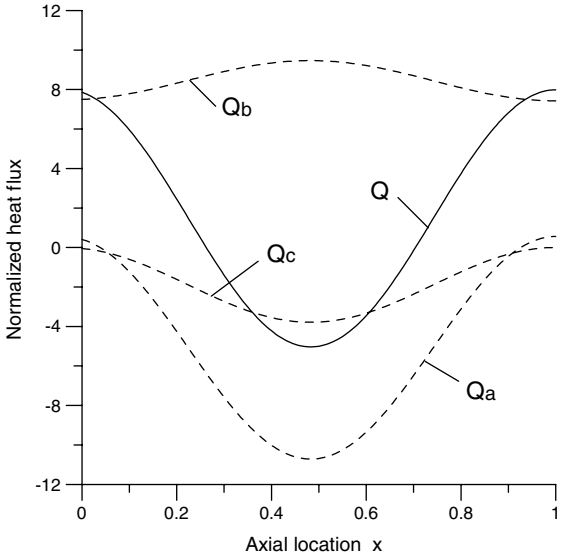

Fig. 7. Local heat transfer rate.

Near two ends of the tube, the energy Q_a needed to drive the cycle-averaged velocity gradient and the kinetic energy loss Q_c are small, whereas the dissipated heat by the local acoustic work is larger than the energy needed to compensate for Q_a and Q_c. Consequently, the rest of the energy has to be discarded in the form of heat in this part of the tube, which is the reason why the total local heat transfer rate is positive near the two ends of the tube as shown in Fig. 7. However, near the center of the tube, the energy needed to drive the cycle-averaged velocity gradient is very large, and the dissipated heat Q_b is not large enough to offset Q_a and Q_c. Consequently, this deficient energy has to be compensated by the local radial heat transfer between the fluid and the wall by absorbing the heat from the wall, or ultimately absorbing the heat from the surrounding environment if the outer wall is at isothermal condition. This is why the total local heat capacity Q is negative near the center of the tube as shown in Fig. 7 and why there is a refrigeration capability for the oscillating flow in such a tube.

From the above analyses, we can conclude that the local heat flux Q_a is a very important term. As we have discussed, the local thermoacoustic energy streaming is contributed by local heat flux Q_a and local acoustic work Q_b. Since the local acoustic work Q_b is positive due to the work input in order to maintain the thermoacoustic fluctuation, hence the local thermoacoustic energy streaming is essentially caused by the local heat flux Q_a, which is the energy required to drive the cycle-averaged axial velocity gradient. On the other hand, as we have discussed, the cycle-averaged velocity is induced by the thermoacoustic mass streaming in order to guarantee mass conservation at a cycle-steady state in a thermoacoustic machine. Therefore, the thermoacoustic mass streaming and energy streaming are intimately connected.

8. Conclusions

In this paper, oscillations of a viscous compressible fluid at cycle steady state in a tube, with an outer isothermal wall and with one end closed and the other end driven by a piston, are analyzed based on a linearized theory. By assuming that the tube is sufficiently long, and the oscillations of the fluid are at a nearly resonant condition with small fluctuation amplitudes, analytical solutions of the first-order quantities are obtained.

(1) From the consideration of global mass conservation at a cycle-steady state, an analytical solution is obtained for the cycle-averaged and cross-sectional averaged axial velocity. It is shown that this average velocity is non-vanishing for a compressible flow due to the mass streaming although the net mass flux being zero everywhere during the cycle-steady state.
(2) It is shown that the cycle-averaged pressure depends on the momentum streaming and friction force. In a tube with a relatively large radius (in comparison with the viscous penetration depth), a conservation relationship between the cycle-averaged pressure and the thermoacoustic momentum streaming is revealed, which is similar in form to the Bernoulli equation in a steady inviscid flow.
(3) Based on the global energy conservation, the total local heat transfer rate is shown to be consisting of local heat flux, local acoustic work and the local work due to the variation of the kinetic energy.
(4) It is shown that the refrigeration effect is mainly caused by the non-vanishing mean velocity as a result of the mass streaming. Therefore, the mass streaming and the energy streaming in a compressible oscillating flow are intimately connected.

References

[1] R. Radebaugh, A review of pulse tube refrigerator, Adv. Cryo. Eng. 35 (1990) 1191–1206.
[2] G.W. Swift, Thermoacoustic engines, J. Acoust. Soc. Am. 84 (4) (1988) 1145–1180.
[3] L. Bauwens, Thermoacoustics: transient regimes and singular temperature profiles, Phys. Fluid 10 (4) (1998) 807–818.
[4] W.E. Gifford, R.C. Longsworth, Surface heat pumping, Adv. Cryo. Eng. 11 (1966) 171–179.

[5] N. Rott, Damped and thermally driven acoustic oscillations in wide and narrow tubes, Z. Angew. Math. Phys. 20 (2) (1969) 230–243.
[6] N. Rott, Thermally driven acoustic oscillations. Part III: Second-order heat flux, Z. Angew. Math. Phys. 26 (1975) 43–49.
[7] N. Rott, Thermoacoustics, Adv. Appl. Mech. 20 (1980) 135–175.
[8] P. Merkli, H. Thomann, Thermoacoustic effects in a resonance tube, J. Fluid Mech. 70 (1975) 161–177.
[9] J.C. Wheatley, T. Hofler, G.W. Swift, A. Nfigliori, An intrinsically irreversible thermoacoustic heat engine, J. Acoust. Soc. Am. 74 (1983) 153–170.
[10] G.W. Swift, Thermoacoustic engines and refrigerators, Phys. Today. 48 (1995) 22–28.
[11] J.H. Xiao, Thermoacoustic heat transportation and energy transformations, Part 2: Isothermal wall thermoacoustic effects, Cryogenics 35 (1995) 21–26.
[12] A.O. Santillán, R.R. Boullosa, Acoustic power and heat fluxes in the thermoacoustic effect due to a travelling plane wave, Int. J. Heat Mass Transfer 40 (1997) 1835–1838.
[13] G.Q. Lu, P. Cheng, Friction factor and Nusselt number for thermoacoustic transport phenomena in a tube, J. Thermophys. Heat Transfer 14 (2000) 566–573.
[14] A. Tominaga, Thermodynamic aspect of thermoacoustic theory, Cryogenics 35 (1995) 427.
[15] A. Gopinath, N.L. Tait, Thermoacoustic streaming in a resonant channel: the time-averaged temperature distribution, J. Acoust. Soc. Am. 103 (1998) 1388–1405.
[16] R. Waxler, Stationary velocity and pressure gradients in a thermoacoustic stack, J. Acoust. Soc. Am. 109 (2001) 2739–2750.
[17] H. Bailliet, V. Gusev, R. Raspet, R.A. Hiller, Acoustic streaming in closed thermoacoustic devices, J. Acoust. Soc. Am. 110 (2001) 1808–1821.
[18] G. Swift, Thermoacoustics: A Unifying Perspective for Some Engines and Refrigerators, The Acoustical Society of America, 2002.
[19] G.Q. Lu, P. Cheng, On cycle-averaged pressure in a G–M type pulse tube refrigerator, Cryogenics 42 (2002) 287–293.
[20] G.Q. Lu, P. Cheng, Numerical and experimental study of a Gifford–McMahon-type pulse tube refrigeration, J. Thermophys. Heat Transfer 17 (2003) 457–463.